



Published in final edited form as:

Crit Care Med. 2014 June ; 42(6): e420–e431. doi:10.1097/CCM.0000000000000309.

Local Burn Injury Impairs Epithelial Permeability and Antimicrobial Peptide Barrier Function in Distal Unburned Skin*

Jennifer K. Plichta, MD^{1,2}, Steve Droho, PhD¹, Brenda J. Curtis, PhD^{1,2}, Parita Patel, BS¹, Richard L. Gamelli, MD^{1,2}, and Katherine A. Radek, PhD^{1,2}

¹Department of Surgery, Burn and Shock Trauma Research Institute, Loyola University Chicago, Health Sciences Division, Maywood, IL

²Department of Surgery, Loyola University Chicago, Health Sciences Division, Maywood, IL

Abstract

Objectives—Our objective was to characterize the mechanisms by which local burn injury compromises epithelial barrier function in burn margin, containing the elements necessary for healing of the burn site, and in distal unburned skin, which serves as potential donor tissue.

Design—Experimental mouse scald burn injury.

Setting—University Research Laboratory.

Subjects—C57/Bl6 Male mice, 8–12 weeks old.

Interventions—To confirm that dehydration was not contributing to our observed barrier defects, in some experiments mice received 1 mL of saline fluid immediately after burn, while a subgroup received an additional 0.5 mL at 4 hours and 1 mL at 24 hours following burn. We then assessed skin pH and transepidermal water loss every 12 hours on the burn wounds for 72 hours postburn.

Measurements and Main Results—Burn margin exhibited increased epidermal barrier permeability indicated by higher pH, greater transepidermal water loss, and reduced lipid synthesis enzyme expression and structural protein production up to 96 hours postburn. By contrast, antimicrobial peptide production and protease activity were elevated in burn margin. Skin extracts from burn margin did not exhibit changes in the ability to inhibit bacterial growth. However, distal unburned skin from burned mice also demonstrated an impaired response to barrier disruption, indicated by elevated transepidermal water loss and reduced lipid synthesis enzyme and structural protein expression up to 96 hours postburn. Furthermore, skin extracts from distal unburned skin exhibited greater protease activity and a reduced capacity to inhibit bacterial growth of several skin pathogens. Finally, we established that antimicrobial peptide levels were

Copyright © 2014 by the Society of Critical Care Medicine and Lippincott Williams & Wilkins

Drs. Plichta, Droho, Gamelli, and Radek designed the research; Drs. Plichta and Droho performed all animal procedures and tissue acquisition; Drs. Plichta, Curtis, and Patel performed the postmortem research; Drs. Plichta and Radek analyzed the data; and all authors were involved in the writing of the article and had final approval of the submitted version.

Supplemental digital content is available for this article. Direct URL citations appear in the printed text and are provided in the HTML and PDF versions of this article on the journal's website (<http://journals.lww.com/ccmjjournal>).

also altered in the lung and bladder, which are common sites of secondary infection in burn-injured patients.

Conclusions—These findings reveal several undefined deficiencies in epithelial barrier function at the burn margin, potential donor skin sites, and organs susceptible to secondary infection. These functional and biochemical data provide novel insights into the mechanisms for graft failure and secondary infection after burn injury.

Keywords

antimicrobial peptides; burn injury; donor skin; lipids; permeability barrier

Intact skin regulates fluid and electrolyte shifts and provides a blockade to external stressors and invading pathogens. The loss of the entire epidermis following traumatic burn injury (TBI) increases morbidity and mortality by promoting severe hemodynamic shock and hematopoietic dysfunction (1-3). Furthermore, third-degree burns involve damage to or complete destruction of the skin and underlying fascia, necessitating skin grafts (4, 5) to avoid infection and fluid loss. In severely burned patients (> 20% total body surface area [TBSA]), autologous grafts from unburned skin frequently exhibit deterioration and functional deficiencies after grafting, suggesting impaired barrier function likely originating from the initial TBI. However, no studies to date have evaluated alterations in physical and chemical variables of cutaneous barrier function in the burn margin or distal donor site as potential mechanisms for graft failure and impaired TBI wound healing.

The epidermis comprises the boundary to the external environment by integrating lipids with structural proteins to create an essentially impermeable barrier. Changes in transepidermal water loss (TEWL) and pH indicate functional disturbances in the skin's protective function and are correlated with both rapid epidermal water loss and dehydration (6, 7). Lipid exocytosis and increased lipid synthesis enzyme activity are two necessary epidermal barrier components (8), which partially depends on coordinated changes in epidermal TEWL and pH to initiate barrier repair (7, 9, 10). Epidermal corneocytes further sustain barrier function by aggregating into highly structured bundles through interactions with the key matrix protein filaggrin (FLG) and surrounding cross-linked cornified envelope proteins, involucrin (IVL) and loricrin (LOR) (10, 11). In addition to lipids and structural proteins, antimicrobial peptides (AMPs) directly maintain epidermal barrier function and inactivate microbes (12, 13). The epidermal serine proteases Kallikrein (KLK) 5 and 7 regulate desquamation as part of normal barrier function (14) and cleave AMP proforms into bioactive peptides (15). Production of cathelicidin (CRAMP) and β -defensin (BD) AMPs is augmented following epithelial barrier disruption, injury, or microbial stimuli (16-19). Other clinically relevant epithelial AMPs include hepcidin (20) and S100A7 (psoriasin) (21). Previous studies in human burn skin and burn blister fluid revealed significant BD reduction compared with unburned subjects (22-24).

The role of skin as a neuroimmune organ has been previously investigated (12, 13, 25-27), but direct support for its ability to elicit global changes in epithelial barrier function after injury is lacking. Evidence suggests that elaborate communication exists between the neuroimmune systems and the skin to balance responses to injury, as components (i.e.,

receptors and ligands) of neuroimmune response pathways are shared and expressed by resident epidermal and dermal cells (9, 28-30). Although skin grafts are obtained from unburned skin (4), the integrity and permeability barrier function at the donor site appear to be compromised compared to skin from unburned patients. Although this phenomenon is widely recognized, the mechanisms behind the deterioration of primary skin grafts after burn injury have not been assessed. Infection and sepsis account for over 50% of all burn-related deaths (31, 32), and impaired barrier function likely contributes to both graft survival and infection/sepsis. The principal discovery of this study is that TBI impairs several epithelial barrier components, on both a functional and molecular level, at the burn margin and in unburned skin, which may be used for grafting. Furthermore, we identified mechanisms by which TBI disrupts epithelial barrier function by evaluating several critical biochemical and functional variables in skin and distal organs that play distinct roles in limiting water loss, stimulating barrier repair, and restricting microbial growth.

MATERIALS AND METHODS

Scald Burn Injury in Mice

A modified burn injury model was employed (33). Eight- to ten-week-old isoflurane anesthetized male C57BL/6 mice (Jackson, Bar Harbor, ME) were plucked 72 hours prior to injury. On the injury day, mice were anesthetized intraperitoneally (i.p.) with ketamine/xylazine, placed in a plastic template exposing 15% TBSA, and subjected to sham (~22°C water for 10 s) or scald burn injury (~92–94°C water for 10 s) to give an insensate full-thickness burn. Mice were resuscitated i.p. with 1 mL of sterile isotonic saline to prevent shock. The burn margin included 5 mm of skin directly adjacent to the burn. Distal skin was harvested from the ventral surface of the mouse. Tissues were harvested 24–96 hours postburn. All animal protocols were approved by the Loyola University Chicago Institutional Animal Care and Use Committee.

Tape-Stripping, TEWL, and pH Assessment

Following sham or burn injury, skin barrier disruption was induced (distal to the dorsal sham/burn injury) by 20 sequential cellophane tape-strippings on the denuded ventral skin (34, 35). Immediate tape-stripping served to assess barrier function over time at potential donor sites up to 3 days postburn, which represents a time point relevant for skin grafting. Delayed tape-stripping at 3 days postburn served to simulate barrier disruption following skin graft harvests from donor sites and meshing during skin grafting procedures (4). TEWL and pH were measured on the ventral and dorsal surfaces of anesthetized mice prior to and between 0 and 96 hours following tapestripping using a TM-300 TEWA meter (Courage-Khazaka, Cologne, Germany) and pH meter. Higher TEWL indicated an abnormal and/or disrupted barrier. Percent changes in pH or TEWL were calculated as follows:

$$\left(\frac{4\text{hr post tape-stripping} - 0\text{hr post tape-stripping}}{0\text{hr post tape-stripping}} \right) \times 100$$

where 0% indicated return to baseline (pre tape-stripping).

High-Pressure Liquid Chromatography Purification and Radial Diffusion Assay

Homogenized skin samples were extracted overnight in 1N acetic acid at 4°C. Acetonitrile high-pressure liquid chromatography (HPLC) peptide separation was performed on a ST 4.6/250-C18 column (Thermo Scientific, Hanover Park, IL). Fractions from each animal were combined, lyophilized, and resuspended in 20 µL of sterile water. Peptide concentrations were normalized and antimicrobial activity evaluated using a radial diffusion assay (36) with 4×10^5 colony-forming units/mL of *Staphylococcus aureus* SA113 (ATCC 35556) wild-type and *mprF* (37), *Streptococcus pyogenes* (ATCC BAA-1633), *Escherichia coli* (ATCC 9637), or *Pseudomonas aeruginosa* (ATCC 19660). Water and catestatin served as negative and positive controls, respectively. Inhibition zones were quantified using ImageJ software (National Institutes of Health, Bethesda, MD).

Histology and Immunohistofluorescence

Immunohistofluorescence (IHF) was performed with antibodies for LOR, IVL, cathelicidin (Abcam, Cambridge, MA), FLG (Covance, Princeton, NJ), BD (Alpha Diagnostics, San Antonio, TX), KLKs (R&D Systems, Minneapolis, MN), and neurofilament M (Millipore, Billerica, MA) (13, 35). In brief, tissues were mounted in optimal cutting temperature medium, then sectioned (8 µm for skin, 5 µm for bladder and lung), fixed in acetone, blocked, incubated overnight at 4°C with primary antibodies, washed, and incubated at room temperature with secondary Cy3 or Alexa Fluor 456 secondary antibodies. Nuclei were stained using Prolong Gold Antifade with 4',6-diamidino-2-phenylindole (Invitrogen-Life Technologies, Grand Island, NY). Micrographs were taken with a 20× objective for skin and lung and 40× objective for bladder. Nile Red staining (38, 39): Frozen sections were expanded using half-strength Sorensen-Walburn buffer for 20 minutes. After adding Nile Red (2.5 µg/mL in 75:25 (vol/vol) glycerol:water), sections were mounted and incubated at 37°C for 1 hour in the dark. All samples were analyzed using 20-fold magnification.

Protease Assays

Protease activity was quantified using the EnzChek Protease Assay kit (Invitrogen-Life Technologies) (40) and normalized by bicinchoninic acid protein assay (Thermo Scientific). Trypsin with and without HALT protease inhibitor (Thermo Scientific) served as controls. Fluorescence was read using a microplate reader and excitation/emission wavelengths of 485/530 nm. Qualitative protease activity was performed with frozen skin sections (8 µm) and nuclei stained as above.

Quantitative Polymerase Chain Reaction

RNA was extracted using Trizol (Invitrogen) and reverse transcribed using iScript cDNA kit (Bio-Rad, Des Plaines, IL). Quantitative polymerase chain reaction (qPCR) was performed using the TaqMan Gene Expression pre-mix (Applied Biosystems, Grand Island, NY) and TaqMan probes (see Supplemental Materials and Methods, Supplemental Digital Content 1, <http://links.lww.com/CCM/A935>). Target genes were normalized to β-actin. Results were analyzed using the 2^{-Ct} method. Fold-changes relative to sham were calculated.

Statistical Analyses

TEWL and pH were calculated as the SEM and analyzed using two-way analysis of variance and Bonferroni posttest. All other data were analyzed independently using two-tailed Student *t* test or Mann-Whitney test. *p* values less than 0.05 were considered statistically significant.

RESULTS

Burn Injury Impairs Permeability Barrier Function, Lipid Synthesis, and Structural Proteins in Burn Margin

To identify early defects in skin barrier function after burn injury, we employed a 15% full-thickness dorsal scald burn injury model or sham injury (33). We first observed a 10–15% increase in epidermal pH within the burn area 24–72 hours following burn, which began to normalize by day 4 (Fig. 1A). The burn area demonstrated a significant TEWL increase for at least 5 days postburn (Fig. 1B). To identify potential mechanisms for these responses, lipid synthesis enzymes crucial for epidermal repair in the burn margin were analyzed. Hydroxymethylglutaryl-CoA reductase (HMGCR), fatty acid synthase (FAS), and serine palmitoyltransferase (SPT) are involved in synthesis of the major extracellular lipids cholesterol, free fatty acids, and ceramide, respectively (6, 8, 41–43). At 24 hours, *FAS* and *HMGCR* gene expression was significantly reduced; *FAS* remained suppressed 96 hours postburn (Fig. 1, C and D). More prominent and diffuse lipid staining after 24 hours was found in burn margin and localized staining in differentiated layers by 96 hours (Fig. 1E). We next investigated whether TEWL and pH changes may be attributed to structural protein defects (10, 13, 44). At 24 hours, both *FLG* and *LOR* gene expression was reduced by more than 50%. While *FLG* normalized by 96 hours, *LOR* remained suppressed (Fig. 1, C and D). Both *FLG* and *IVL* protein levels were enhanced in differentiated epidermis at 24 hours, while *LOR* was markedly reduced. By 96 hours, *FLG* and *LOR* levels normalized. However, *IVL* localization was greater in the basal rather than the differentiated epidermal layer (Fig. 1E).

Burn Injury Alters Local AMPs and Protease Activity in Burn Margin

We next characterized production and localization of AMPs necessary for maintaining skin barrier function (13) and pathogen defense (18) in burn margin and sham. *Cramp* gene expression was significantly increased, while *s100A7* was reduced after 24 hours (Fig. 2A). At 96 hours, *s100A7* and *HAMP2* were suppressed, whereas *DefB3* and *DefB14* were elevated (Fig. 2B). CRAMP and mBD3 protein production was more robust throughout the entire epidermis at 24 hours, but normalized by 96 hours (Fig. 2C). To investigate whether the altered epidermal AMP production alters the skin's capacity to inhibit the growth of common burn-related pathogens, burn margin isolated at 96 hours postburn was subjected to HPLC and subsequent antimicrobial assay, as this time point is considered clinically relevant for wound debridement and infection susceptibility. Although not statistically significant, we observed a ~50% reduction in *E. coli* inhibition ($p = 0.06$) (Fig. 2D). This paralleled reduced *s100A7* that is known to selectively kill *E. coli* (21) (Fig. 2, A and B). The activity of burn-injured and sham skin did not significantly differ against other skin pathogens.

Since KLK5 and 7 are essential for desquamation, cohesion, and AMP activation (15, 28, 45), we speculated that they participate in burn margin barrier defects. *KLK5* and *KLK7* expression was reduced by greater than 70% 24 hours postburn and normalized by 96 hours (Fig. 3A). We observed greater *KLK5* abundance within the stratum corneum 24 hours postburn (Fig. 3B) and noted a robust and diffuse *KLK7* localization in the granular layers and stratum corneum compared to sham. No differences were observed at 96 hours. A significant functional total protease activity increase 24 hours in burned skin compared to sham was observed (Fig. 3C). This effect was lost when normalized to total protein, indicating greater total protein likely from infiltrating inflammatory cells and cellular debris following burn. We localized the protease activity increase to the granular epidermis layer and the reticular dermis at 24 hours; by 96 hours postburn, total protease activity remained diffusely elevated in the epidermis and dermis (Fig. 3E).

Local Burn Injury Alters Barrier Function and Recovery in Distal Unburned Skin

Because epidermal barrier function impairment at the donor site could potentially elicit wound healing defects at the injury site, we compared barrier defects in burn margin with unburned skin. Mice were subjected to tape-stripping of skin distal to the site of dorsal sham or burn immediately following or 3 days postburn or sham injury to assess responses to barrier disruption at a time point relevant for skin grafting. The delayed tape-stripping simulates barrier disruption following skin graft harvests from donor sites and meshing during skin grafting procedures (4). Immediate tape-stripping after burn dampened the response to barrier disruption, characterized by lower TEWL 4–24 hours postburn (Fig. 4A). By contrast, delayed tape-stripping following burn exaggerated the response, yielding significantly greater TEWL up to 12 hours post-tape-stripping (Fig. 4B). To investigate whether the exacerbated response following delayed tape-stripping in burned mice would dampen the essential lipid synthesis enzyme increase in distal (non-tape-stripped) skin, we performed qPCR and identified a significant *HMGCR* reduction 24 hours postburn, which normalized by 96 hours (Fig. 4, C and D); no significant differences in *FAS* or *SPT* expression were identified.

We then investigated baseline lipid distribution and structural proteins in distal, non-tape-stripped skin. Diffuse extracellular lipid staining was highly concentrated at the interface between stratum corneum and stratum granulosum of sham mouse skin (Fig. 4E). However, distal skin from burned mice exhibited a loss of stratified lipid deposition and prominence of more globular lipids in the outermost stratum corneum layer. At 96 hours postburn, the lipids appeared more concentrated in the outer differentiated epidermal layers (Fig. 4E). *IVL* expression in distal, unburned skin from burn-injured mice was substantially greater at 24 hours (Fig. 4C), whereas *FLG* was significantly reduced at 96 hours (Fig. 4D) compared to sham. *FLG* protein in distal unburned skin was less prominent in the differentiated epidermal layers 24 hours postburn, but returned to sham levels by 96 hours. *IVL* and *LOR* protein localization in distal skin was unchanged (Fig. 4E).

Local Burn Injury Impairs AMP and Protease Activity in Distal unburned Skin

We evaluated whether potential donor skin from unburned sites exhibits normal AMP levels and activity. Only *DefBI* expression was significantly reduced 24 hours postburn, which

normalized by 96 hours (Fig. 5, A and B). CRAMP and mBD3 proteins were robustly elevated 24 hours postburn and normalized by 96 hours (Fig. 5C). Distal, unburned skin demonstrated diminished antimicrobial activity against skin pathogens, including *S. aureus* and *P. aeruginosa*. No significant changes were observed for *S. pyogenes* or *E. coli* (Fig. 5D). Since AMPs are also critical for barrier function and microbial defense in lung and bladder (46-49), we investigated whether burn injury elicits global AMP regulation defects in these common sites for secondary infection. Although the gene expression of most investigated AMPs in the bladder was not significantly altered at 24 hours, *DefB1*, *DefB3*, *DefB14*, *HAMP1*, *HAMP2*, and *s100A7* levels were markedly reduced after 96 hours (Fig. S1A-B, Supplemental Digital Content 2, <http://links.lww.com/CCM/A936>). *HAMP1* protein levels were more prevalent in the epithelial layers at both 24 and 96 hours postburn compared to sham (Fig. S1C, Supplemental Digital Content 2, <http://links.lww.com/CCM/A936>). In the lung, *DefB14* was significantly reduced at 24 hours, whereas *Cramp* was substantially increased (Fig. S2A, Supplemental Digital Content 3, <http://links.lww.com/CCM/A937>). *HAMP2* was significantly reduced at both time points (Fig. S2A-B, Supplemental Digital Content 3, <http://links.lww.com/CCM/A937>). CRAMP protein levels were slightly lower in lung epithelia at 24 hours postburn and further diminished by 96 hours (Fig. S2C, Supplemental Digital Content 3, <http://links.lww.com/CCM/A937>).

To determine if AMP reduction may be partly mediated by alterations in epidermal protease activity, we quantified *KLK5* and *KLK7*. *KLK5* gene expression in distal unburned skin was substantially reduced at 24 hours. A similar trend was observed for *KLK7*; both normalized by 96 hours (Fig. 6A). No considerable differences were noted for *KLK* protein production or localization (Fig. 6B). The overall distal skin protease activity was significantly increased 24 and 96 hours postburn (Fig. 6, C and D). In contrast to burned injured skin, the increase in protease activity in distal unburned skin did not correlate with a global total protein increase, since these changes were still observed following normalization to total protein. Concordant findings were demonstrated for overall protease activity, which revealed an increase in dermal protease activity (Fig. 6E).

DISCUSSION

Normal epidermal barrier permeability is crucial for hemodynamic stability, optimal wound healing, graft survival, and pathogen resistance after TBI. A recent case study revealed that evaporative skin heat loss was substantially diminished in a burn patient who had undergone 75% TBSA skin grafting compared to unburned controls, providing direct evidence that unburned autologous donor skin exhibits functional deficits related to heat stress (29). Our study is the first identifying compromised variables of skin barrier function after TBI, potential mechanisms by which these defects occur, and a global AMP barrier function defect. We found that TEWL and pH elevations in burn-injured and distal unburned skin are sustained for several days following TBI, which correlated with cutaneous barrier impairment. The prolonged increase in barrier permeability and pH could potentially hinder barrier recovery and graft survival following wound debridement and subsequent grafting of donor skin. We speculate that traumatic skin burn injury likely elicits a more robust response to barrier disruption locally, which may overwhelm the normal barrier recovery response.

In contrast to other barrier disruption studies (8, 11, 35), we observed a decrease in both *FAS* and *HMGCR* lipid synthesis enzyme expression in burn margin and distal skin, although TEWL remained elevated. This paralleled epidermal lipid redistribution in burn margin and distal unburned skin, indicating a lipid synthesis shift. In addition, burn injury elicited systemic effects seen as altered distal response to barrier disruption (i.e., tape-stripping) in potential donor skin. The abnormal TEWL changes following distal tape-stripping in burned mice, which mimics barrier disruption of split-thickness grafts using meshing procedures, were similarly associated with lipid synthesis enzyme suppression. Perhaps a TEWL threshold exists to determine the initiation and extent of lipid-dependent barrier recovery, which is contingent upon barrier disruption severity. One mechanism for this may be reduced cholesterol and fatty acid availability necessary for extracellular lamellar membranes that comprise the epidermal permeability barrier. Sterol regulatory element binding protein (SREBP)-2 was identified as the predominant epidermal SREBP, and higher SREBP-2 levels corresponded with an increase in specific cholesterol and fatty acid synthetic enzyme expression (i.e., *FAS* and *HMGCR*, respectively), but not for ceramide synthesis enzymes (i.e., *SPT*) (30). Since we observed a significant *FAS* and *HMGCR* reduction in burn margin and distal unburned skin, we speculate that TBI may be altering the transcriptional regulation of these lipid synthesizing enzymes through SREBP-2 or similar transcriptional elements ultimately impairing normal barrier function and recovery.

Dermal neuronal signaling is likely playing a lesser role in these responses, as we histologically confirmed full-thickness burn and denervation following burn (Fig. S3, Supplemental Digital Content 4, <http://links.lww.com/CCM/A938>; Fig. S4, Supplemental Digital Content 5, <http://links.lww.com/CCM/A939>; Fig. S5, Supplemental Digital Content 6, <http://links.lww.com/CCM/A940>). Furthermore, we confirmed that TEWL and epidermal barrier changes were not solely due to rapid dehydration, as similar alterations were observed in mice receiving standard or additional resuscitation following burn (Fig. S6, Supplemental Digital Content 7, <http://links.lww.com/CCM/A941>). Since epidermal hydration allows for flexibility in a healthy state, increased epidermal barrier permeability can also make the skin less malleable during grafting procedures. Disturbances in calcium or potassium gradients also inhibit lamellar body secretion to restore normal permeability barrier function (31, 32), which may be the case after burn injury due to changes in blood volume and hydration.

Several dermatoses have been linked to a genetic *LOR* mutation disturbing cornified envelope formation (50, 51) or consistently lower epidermal *LOR* production ultimately promoting barrier deficiencies (52, 53). *FLG* deficiency, genetic mutation, and defective processing also correlate with epidermal barrier diseases, including psoriasis and atopic dermatitis (53-55). Our data are consistent with these studies involving skin pathologies of a noninjurious nature and suggest that TBI similarly disrupts the abundance and localization of the key structural proteins—*FLG*, *LOR*, and *IVL*—in a spacial-temporal fashion to increase barrier permeability. It is plausible that desmosomal proteins, such as desmoplakin, desmoglein-1, and desmoglein-3, and the tight junction protein, zona occludens-1, may also be influenced by TBI in both the burn margin and distal unburned skin, as these proteins are critical for epidermal development (6, 14, 56) and warrant further investigation.

Significant burn injuries are known to induce a prolonged state of immunosuppression, which further predisposes burn patients to lung and urinary tract infections (57). Given the massive amount of stressors after traumatic injury, the defect in the ability of distal unburned skin to restrict bacterial growth via aberrant AMP production and responses may partially explain the high infection prevalence in burn patients. Our observations of impaired AMP production in distal skin, lung, and bladder can presumably increase barrier permeability to facilitate microbial colonization or be the source of bacterial dissemination into the skin wound or other organs. Similar to the epidermal structural proteins, our findings suggest divergent temporal and spacial AMP regulation at the gene and protein levels.

Although KLK gene expression was reduced in burn margin and distal skin after injury, the observed KLK protein increase is more likely due to the release of prestored proteases within epidermal lamellar bodies. These findings correlated with the increase in functional protease activity and suggest divergent transcriptional and translational KLK5 and 7 regulation. Acute barrier disruption correlates with greater serine protease activity (such as KLKs) (14, 28) and blockade with serine protease inhibitors accelerates barrier recovery related to elevated lamellar body secretion via protease-activated receptor-2 (58). Since a pH gradient exists in human skin (9), we speculate that the skin pH increase after burn can exert several deleterious effects on barrier permeability by increasing serine protease activity, resulting in AMP inactivation or degradation (10). The elevated pH levels after burn injury provide a likely mechanism for increased protease activity in both burn margin and distal skin, which can be explained by the hemodynamic and electrolyte imbalance caused by the burn.

Collectively, our data indicate that burn injury disrupts epithelial barrier function by lipid, structural protein, AMP, and protease modulation at the primary injury site and in distal skin and organs. These findings may facilitate new treatments to improve the functionality of burn wounds, repeatedly used autograft sites, and skin flap procedures. The limited availability of autologous skin in severely burned patients requires that donor skin be repeatedly excised from the same site over the course of multiple grafting procedures. Thus, impaired epithelial barrier function due to altered lipid, AMP, or protease activity will likely have implications for hemodynamic stability, wound healing, graft survival, and microbial defense. Our data suggest that early, targeted therapy designed to improve epithelial barrier function at the primary burn margin site and potential donor sites prior to grafting will likely improve patient outcomes and graft survival. We are currently investigating whether skin barrier defects also occur in human burns and the clinical aspects that may be influencing these variables.

Supplementary Material

Refer to Web version on PubMed Central for supplementary material.

Acknowledgments

We thank Dr. Ravi Shankar for his respected expertise and valuable insight, and Dr. Sascha Kristian for editing the article.

Drs. Plichta, Droho, Patel, Gamelli, and Radek (NIH T32-GM008750-11) received support for article research from the National Institutes of Health (NIH). Their institutions received grant support from the NIH. Dr. Curtis received salary support and support for travel from an NIH grant (T32 5T32AA013527-09). She received support for article research from the NIH. Her institution received grant support from the NIH. Drs. Gamelli and Radek were supported by Dr. Ralph and Marian C. Falk Medical Research Trust.

REFERENCES

1. Molina PE. Neurobiology of the stress response: Contribution of the sympathetic nervous system to the neuroimmune axis in traumatic injury. *Shock*. 2005; 24:3–10. [PubMed: 15988314]
2. Baxter CR. Fluid volume and electrolyte changes of the early postburn period. *Clin Plast Surg*. 1974; 1:693–703. [PubMed: 4609676]
3. Loebl EC, Baxter CR, Curreri PW. The mechanism of erythrocyte destruction in the early post-burn period. *Ann Surg*. 1973; 178:681–686. [PubMed: 4759400]
4. Alexander JW, MacMillan BG, Law E, et al. Treatment of severe burns with widely meshed skin autograft and meshed skin allograft overlay. *J Trauma*. 1981; 21:433–438. [PubMed: 7230295]
5. Phillips TJ, Gilchrest BA. Clinical applications of cultured epithelium. *Epithelial Cell Biol*. 1992; 1:39–46. [PubMed: 1307936]
6. Proksch E, Brandner JM, Jensen JM. The skin: An indispensable barrier. *Exp Dermatol*. 2008; 17:1063–1072. [PubMed: 19043850]
7. Feingold KR, Schmuth M, Elias PM. The regulation of permeability barrier homeostasis. *J Invest Dermatol*. 2007; 127:1574–1576. [PubMed: 17568800]
8. Proksch E, Holleran WM, Menon GK, et al. Barrier function regulates epidermal lipid and DNA synthesis. *Br J Dermatol*. 1993; 128:473–482. [PubMed: 8504036]
9. Hachem JP, Crumrine D, Fluhr J, et al. pH directly regulates epidermal permeability barrier homeostasis, and stratum corneum integrity/cohesion. *J Invest Dermatol*. 2003; 121:345–353. [PubMed: 12880427]
10. Elias PM. Stratum corneum defensive functions: An integrated view. *J Invest Dermatol*. 2005; 125:183–200. [PubMed: 16098026]
11. Ekanayake-Mudiyanselage S, Aschauer H, Schmook FP, et al. Expression of epidermal keratins and the cornified envelope protein involucrin is influenced by permeability barrier disruption. *J Invest Dermatol*. 1998; 111:517–523. [PubMed: 9740250]
12. Elias PM. The skin barrier as an innate immune element. *Semin Immunopathol*. 2007; 29:3–14. [PubMed: 17621950]
13. Aberg KM, Man MQ, Gallo RL, et al. Co-regulation and interdependence of the mammalian epidermal permeability and antimicrobial barriers. *J Invest Dermatol*. 2008; 128:917–925. [PubMed: 17943185]
14. Caubet C, Jonca N, Brattsand M, et al. Degradation of corneodesmosome proteins by two serine proteases of the kallikrein family, SCTE/KLK5/hK5 and SCCE/KLK7/hK7. *J Invest Dermatol*. 2004; 122:1235–1244. [PubMed: 15140227]
15. Yamasaki K, Schaubert J, Coda A, et al. Kallikrein-mediated proteolysis regulates the antimicrobial effects of cathelicidins in skin. *FASEB J*. 2006; 20:2068–2080. [PubMed: 17012259]
16. Ahrens K, Schunck M, Podda GF, et al. Mechanical and metabolic injury to the skin barrier leads to increased expression of murine beta-defensin-1, -3, and -14. *J Invest Dermatol*. 2011; 131:443–452. [PubMed: 20944649]
17. Dorschner RA, Pestonjamas VK, Tamakuwala S, et al. Cutaneous injury induces the release of cathelicidin anti-microbial peptides active against group A *Streptococcus*. *J Invest Dermatol*. 2001; 117:91–97. [PubMed: 11442754]
18. Nizet V, Ohtake T, Lauth X, et al. Innate antimicrobial peptide protects the skin from invasive bacterial infection. *Nature*. 2001; 414:454–457. [PubMed: 11719807]
19. Schaubert J, Dorschner RA, Coda AB, et al. Injury enhances TLR2 function and antimicrobial peptide expression through a vitamin D-dependent mechanism. *J Clin Invest*. 2007; 117:803–811. [PubMed: 17290304]

20. Verga Falzacappa MV, Muckenthaler MU. Hecpudin: Iron-hormone and anti-microbial peptide. *Gene*. 2005; 364:37–44. [PubMed: 16203112]
21. Gläser R, Harder J, Lange H, et al. Antimicrobial psoriasin (S100A7) protects human skin from *Escherichia coli* infection. *Nat Immunol*. 2005; 6:57–64. [PubMed: 15568027]
22. Milner SM, Ortega MR. Reduced antimicrobial peptide expression in human burn wounds. *Burns*. 1999; 25:411–413. [PubMed: 10439149]
23. Ortega MR, Ganz T, Milner SM. Human beta defensin is absent in burn blister fluid. *Burns*. 2000; 26:724–726. [PubMed: 11024605]
24. Poindexter BJ, Bhat S, Buja LM, et al. Localization of antimicrobial peptides in normal and burned skin. *Burns*. 2006; 32:402–407. [PubMed: 16621313]
25. Martin-Ezquerria G, Man MQ, Hupe M, et al. Psychological stress regulates antimicrobial peptide expression by both glucocorticoid and beta-adrenergic mechanisms. *Eur J Dermatol*. 2011; 21(Suppl 2):48–51. [PubMed: 21628130]
26. Radek KA. Antimicrobial anxiety: The impact of stress on antimicrobial immunity. *J Leukoc Biol*. 2010; 88:263–277. [PubMed: 20442225]
27. Lopez NE, Krzyzaniak M, Costantini TW, et al. Vagal nerve stimulation blocks peritoneal macrophage inflammatory responsiveness after severe burn injury. *Shock*. 2012; 38:294–300. [PubMed: 22683732]
28. Brattsand M, Stefansson K, Lundh C, et al. A proteolytic cascade of kallikreins in the stratum corneum. *J Invest Dermatol*. 2005; 124:198–203. [PubMed: 15654974]
29. Ganio MS, Gagnon D, Stapleton J, et al. Effect of human skin grafts on whole-body heat loss during exercise heat stress: A case report. *J Burn Care Res*. 2013; 34:e263–e270. [PubMed: 23202874]
30. Harris IR, Farrell AM, Holleran WM, et al. Parallel regulation of sterol regulatory element binding protein-2 and the enzymes of cholesterol and fatty acid synthesis but not ceramide synthesis in cultured human keratinocytes and murine epidermis. *J Lipid Res*. 1998; 39:412–422. [PubMed: 9508001]
31. Denda M, Fuziwara S, Inoue K. Influx of calcium and chloride ions into epidermal keratinocytes regulates exocytosis of epidermal lamellar bodies and skin permeability barrier homeostasis. *J Invest Dermatol*. 2003; 121:362–367. [PubMed: 12880429]
32. Elias PM, Nau P, Hanley K, et al. Formation of the epidermal calcium gradient coincides with key milestones of barrier ontogenesis in the rodent. *J Invest Dermatol*. 1998; 110:399–404. [PubMed: 9540982]
33. Faunce DE, Gregory MS, Kovacs EJ. Effects of acute ethanol exposure on cellular immune responses in a murine model of thermal injury. *J Leukoc Biol*. 1997; 62:733–740. [PubMed: 9400814]
34. Wood LC, Jackson SM, Elias PM, et al. Cutaneous barrier perturbation stimulates cytokine production in the epidermis of mice. *J Clin Invest*. 1992; 90:482–487. [PubMed: 1644919]
35. Curtis BJ, Plichta JK, Blatt H, et al. Nicotinic acetylcholine receptor stimulation impairs epidermal permeability barrier function and recovery and modulates cornified envelope proteins. *Life Sci*. 2012; 91:1070–1076. [PubMed: 22940618]
36. Radek KA, Elias PM, Taupenot L, et al. Neuroendocrine nicotinic receptor activation increases susceptibility to bacterial infections by suppressing antimicrobial peptide production. *Cell Host Microbe*. 2010; 7:277–289. [PubMed: 20413096]
37. Peschel A, Jack RW, Otto M, et al. *Staphylococcus aureus* resistance to human defensins and evasion of neutrophil killing via the novel virulence factor MprF is based on modification of membrane lipids with l-lysine. *J Exp Med*. 2001; 193:1067–1076. [PubMed: 11342591]
38. Fowler SD, Greenspan P. Application of Nile red, a fluorescent hydrophobic probe, for the detection of neutral lipid deposits in tissue sections: Comparison with oil red O. *J Histochem Cytochem*. 1985; 33:833–836. [PubMed: 4020099]
39. Greenspan P, Mayer EP, Fowler SD. Nile red: A selective fluorescent stain for intracellular lipid droplets. *J Cell Biol*. 1985; 100:965–973. [PubMed: 3972906]
40. Menges DA, Ternullo DL, Tan-Wilson AL, et al. Continuous assay of proteases using a microtiter plate fluorescence reader. *Anal Biochem*. 1997; 254:144–147. [PubMed: 9398357]

41. Baroni A, Buommino E, De Gregorio V, et al. Structure and function of the epidermis related to barrier properties. *Clin Dermatol.* 2012; 30:257–262. [PubMed: 22507037]
42. Holleran WM, Man MQ, Gao WN, et al. Sphingolipids are required for mammalian epidermal barrier function. Inhibition of sphingolipid synthesis delays barrier recovery after acute perturbation. *J Clin Invest.* 1991; 88:1338–1345. [PubMed: 1918384]
43. Harris IR, Farrell AM, Grunfeld C, et al. Permeability barrier disruption coordinately regulates mRNA levels for key enzymes of cholesterol, fatty acid, and ceramide synthesis in the epidermis. *J Invest Dermatol.* 1997; 109:783–787. [PubMed: 9406821]
44. Jackson SM, Williams ML, Feingold KR, et al. Pathobiology of the stratum corneum. *West J Med.* 1993; 158:279–285. [PubMed: 8460510]
45. Brattsand M, Egelrud T. Purification, molecular cloning, and expression of a human stratum corneum trypsin-like serine protease with possible function in desquamation. *J Biol Chem.* 1999; 274:30033–30040. [PubMed: 10514489]
46. Doss M, White MR, Teclé T, et al. Human defensins and LL-37 in mucosal immunity. *J Leukoc Biol.* 2010; 87:79–92. [PubMed: 19808939]
47. Parameswaran GI, Sethi S, Murphy TF. Effects of bacterial infection on airway antimicrobial peptides and proteins in COPD. *Chest.* 2011; 140:611–617. [PubMed: 21349930]
48. Tsai PW, Yang CY, Chang HT, et al. Human antimicrobial peptide LL-37 inhibits adhesion of *Candida albicans* by interacting with yeast cell-wall carbohydrates. *PLoS One.* 2011; 6:e17755. [PubMed: 21448240]
49. Lavelle JP, Apodaca G, Meyers SA, et al. Disruption of guinea pig urinary bladder permeability barrier in noninfectious cystitis. *Am J Physiol.* 1998; 274:F205–F214. [PubMed: 9458841]
50. Maestrini E, Monaco AP, McGrath JA, et al. A molecular defect in loricrin, the major component of the cornified cell envelope, underlies Vohwinkel's syndrome. *Nat Genet.* 1996; 13:70–77. [PubMed: 8673107]
51. Ishida-Yamamoto A, McGrath JA, Lam H, et al. The molecular pathology of progressive symmetric erythrokeratoderma: A frameshift mutation in the loricrin gene and perturbations in the cornified cell envelope. *Am J Hum Genet.* 1997; 61:581–589. [PubMed: 9326323]
52. Jensen JM, Fölster-Holst R, Baranowsky A, et al. Impaired sphingomyelinase activity and epidermal differentiation in atopic dermatitis. *J Invest Dermatol.* 2004; 122:1423–1431. [PubMed: 15175033]
53. Kim BE, Howell MD, Guttman-Yassky E, et al. TNF-alpha downregulates filaggrin and loricrin through c-Jun N-terminal kinase: Role for TNF-alpha antagonists to improve skin barrier. *J Invest Dermatol.* 2011; 131:1272–1279. [PubMed: 21346775]
54. Irvine AD, McLean WH, Leung DY. Filaggrin mutations associated with skin and allergic diseases. *N Engl J Med.* 2011; 365:1315–1327. [PubMed: 21991953]
55. Gruber R, Elias PM, Crumrine D, et al. Filaggrin genotype in ichthyosis vulgaris predicts abnormalities in epidermal structure and function. *Am J Pathol.* 2011; 178:2252–2263. [PubMed: 21514438]
56. Kurzen H, Henrich C, Booken D, et al. Functional characterization of the epidermal cholinergic system in vitro. *J Invest Dermatol.* 2006; 126:2458–2472. [PubMed: 16810300]
57. American Burn Association. 2012 National Burn Repository: Report of Data from 2002-2012. American Burn Association; Chicago, IL: 2012.
58. Hachem JP, Houben E, Crumrine D, et al. Serine protease signaling of epidermal permeability barrier homeostasis. *J Invest Dermatol.* 2006; 126:2074–2086. [PubMed: 16691196]

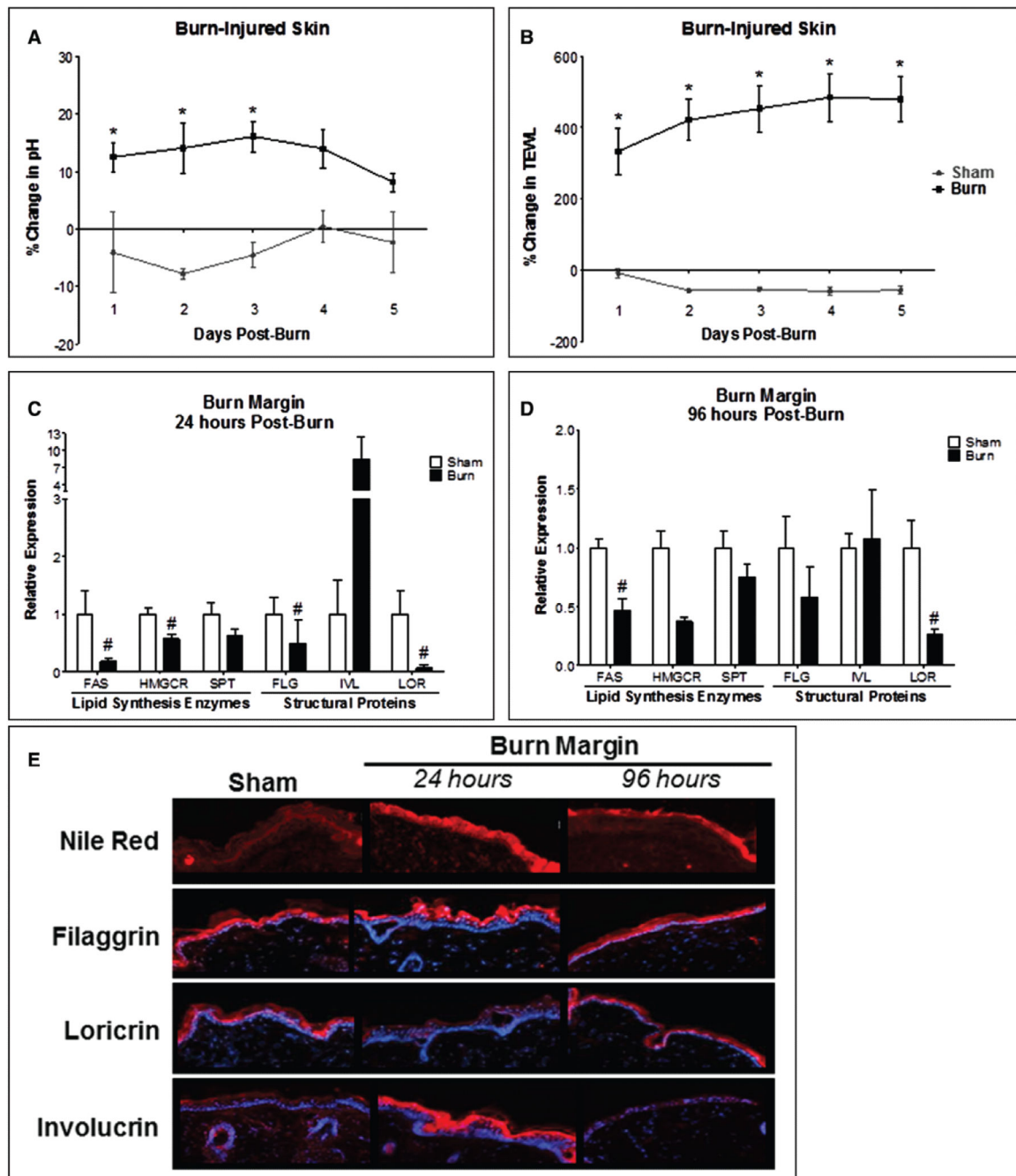


Figure 1.

Burn injury alters the local functional and structural components of the cutaneous barrier. Following scald burn injury, pH (A) and transepidermal water loss (TEWL) (B) were measured daily for 5 days postburn. $n = 4-7$ mice/group. Data analyzed by two-way analysis of variance, Bonferroni posttest ($*p < 0.05$). Mice were euthanized at 24 and 96 hr postburn. Burn margin at 24 hr (C) and 96 hr (D) postburn analyzed for gene expression of lipid synthesis enzymes (fatty acid synthase [FAS], hydroxymethylglutaryl-CoA reductase [HMGCR], and serine palmitoyltransferase [SPT]) and structural proteins (filaggrin [FLG],

involucrin [IVL], and loricrin [LOR]). $n = 6-9$ samples/group, experiments performed in duplicate. Data analyzed by unpaired t test ($\#p < 0.05$) or Mann-Whitney test. **E**, Burn margin at 24 and 96 hr stained for lipids by Nile Red and for FLG, IVL, and LOR by immunohistofluorescence. $n = 3-4$ samples/group.

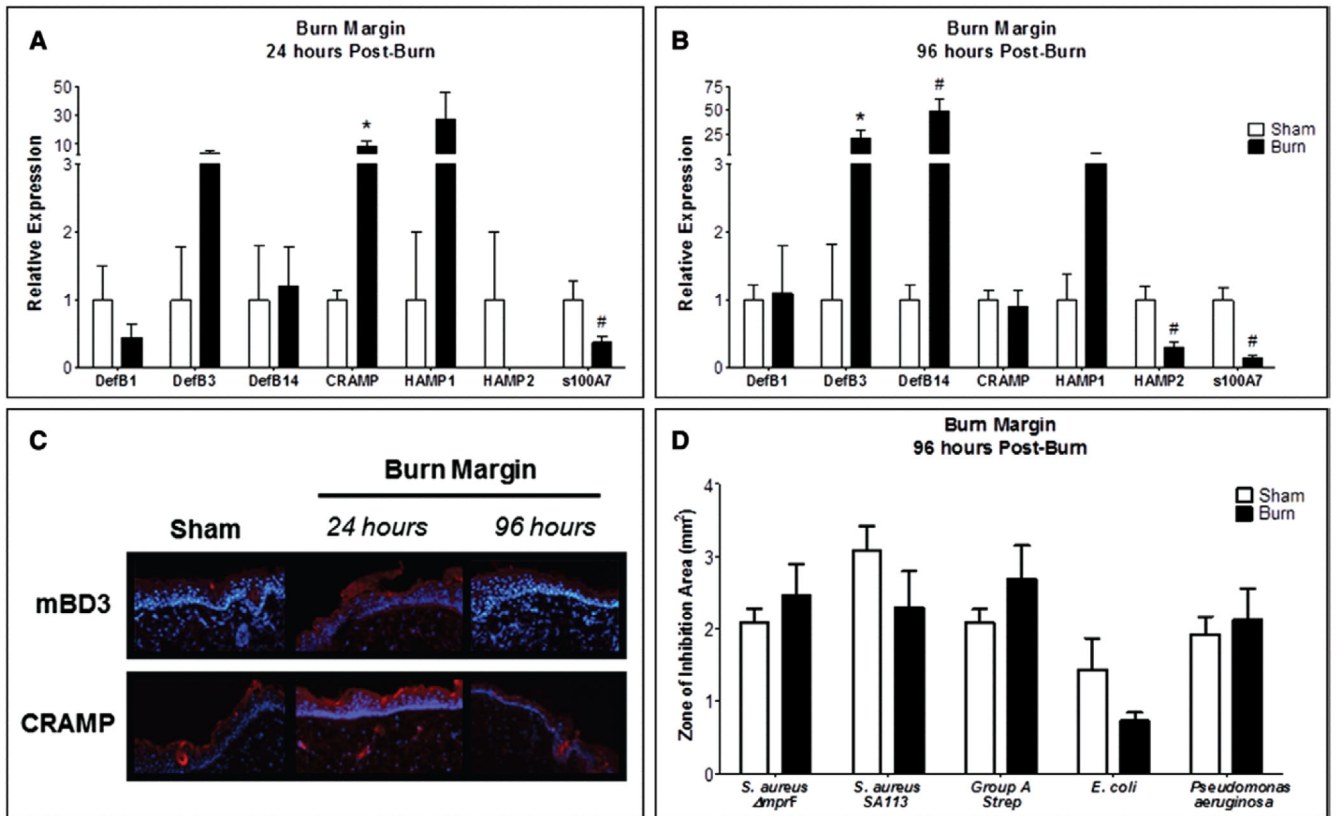


Figure 2.

Burn injured skin promotes divergent modulation of antimicrobial peptides but does not alter local bacterial growth inhibition. Gene expression of *DefB1*, *DefB3*, *DefB14*, *Cramp*, *HAMP1*, *HAMP2*, and *s100A7* in burn margin at 24 hr (A) and 96 hr (B) postburn. $n = 3-9$ samples/group and performed in duplicate. Data analyzed by Mann-Whitney ($*p < 0.05$) and unpaired t test ($\#p < 0.05$). C, Burn margin was stained by immunohistofluorescence for mouse β -defensin 3 (mBD3) and cathelicidin-related antimicrobial peptide (CRAMP). $n = 3-4$ samples/group. D, Burn margin was harvested 96 hr postburn and subjected to high-pressure liquid chromatography fractionation and radial diffusion assay. Bacterial growth inhibition was assessed for using ImageJ software. $n = 3-7$ samples/group. Data analyzed by unpaired t test.

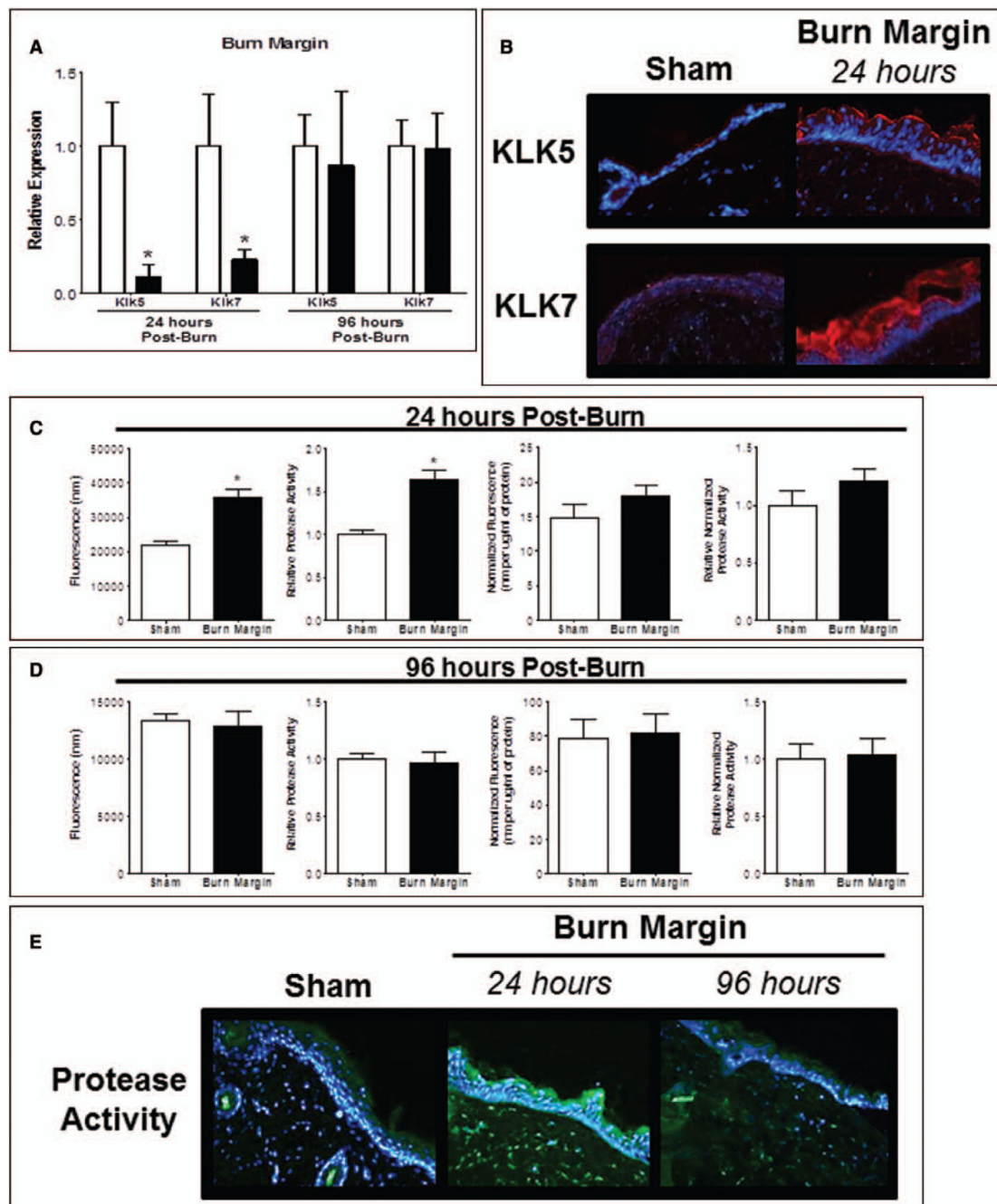


Figure 3.

Burn injury alters protease activity in burn injured skin. **A**, Gene expression of kallikrein (*KLK*) 5 and *KLK*7 in burn margin at 24 and 96 hr postburn. $n = 3-7$ samples/group and performed in duplicate. Data analyzed by unpaired t test ($*p < 0.05$). **B**, Burn margin was stained by immunohistofluorescence (IHF) for *KLK*5 and *KLK*7 at 24 hr postburn. $n = 3-4$ samples/group. Protease activity at 24 hr (**C**) and 96 hr (**D**) postburn using the EnzChek Protease Assay. Data expressed as raw fluorescence observed and normalized to protein concentration. $n = 6-7$ samples/group and experiments performed in duplicate. Data

analyzed by unpaired *t* test ($*p < 0.05$). **E**, Protease activity in burn margin at 24 and 96 hr postburn by IHF. *n* = 3–4 samples/group.

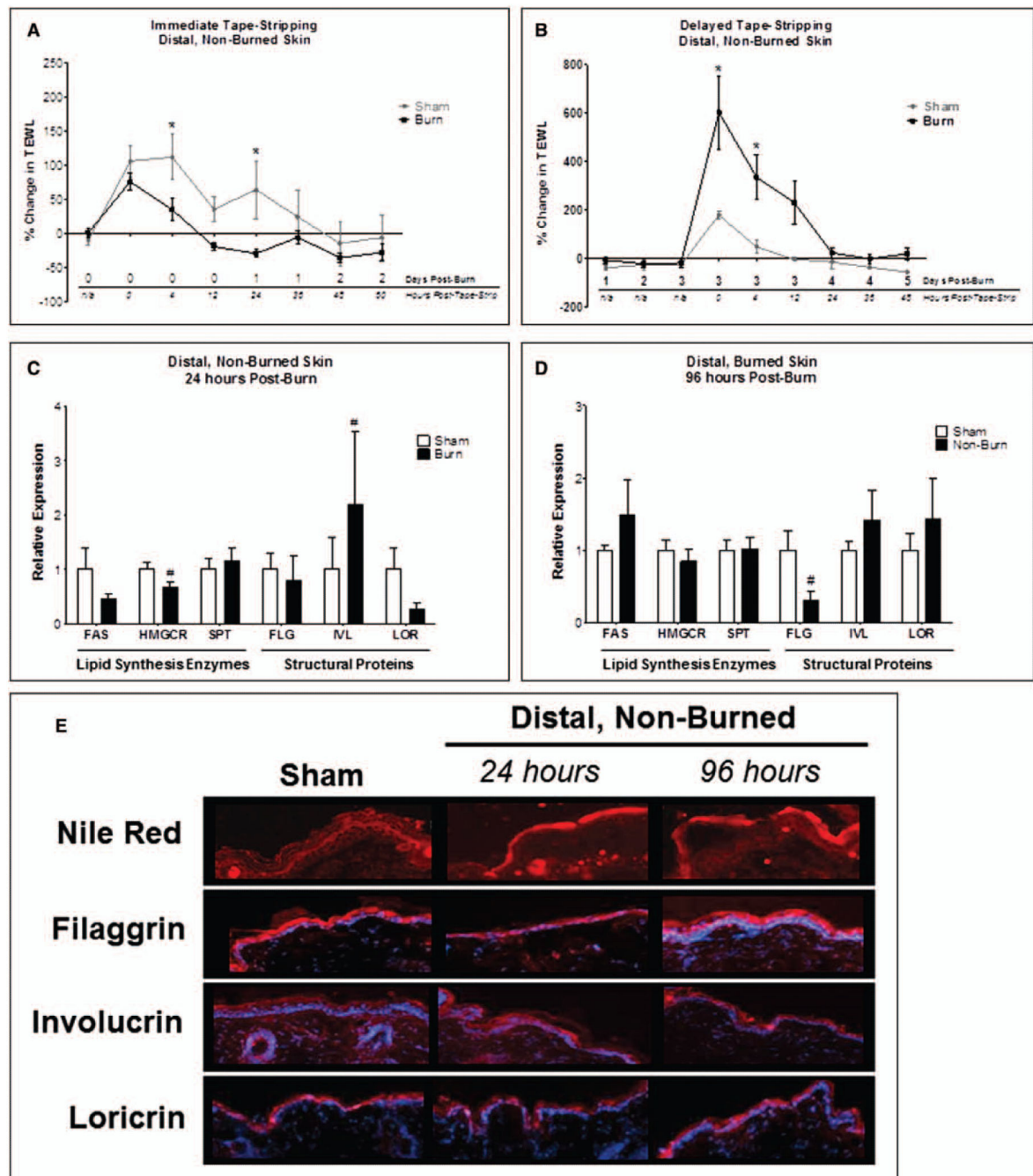


Figure 4.

Local burn injury impairs epidermal permeability barrier function and the response to barrier disruption in distal, unburned skin. Distal (unburned) skin subjected to tape-stripping immediately after burn (A) or 3 days postburn (B) and transepidermal water loss (TEWL) was measured. $n = 4-6$ mice/group. Data analyzed by two-way analysis of variance and Bonferroni posttest ($*p < 0.05$). Distal skin at 24 hr (C) and 96 hr (D) postburn analyzed for gene expression of lipid synthesis enzymes (fatty acid synthase [FAS], hydroxymethylglutaryl-CoA reductase [HMGCR], and serine palmitoyltransferase [SPT])

and structural proteins (filaggrin [FLG], involucrin [IVL], and loricrin [LOR]). $n = 6-8$ samples/group. Data analyzed by unpaired t test or Mann-Whitney test ($\#p < 0.05$). **E**, Distal skin at 24 and 96 hr postburn stained for lipids by Nile Red and for FLG, IVL, and LOR by immunohistofluorescence. $n = 3-4$ samples/group.

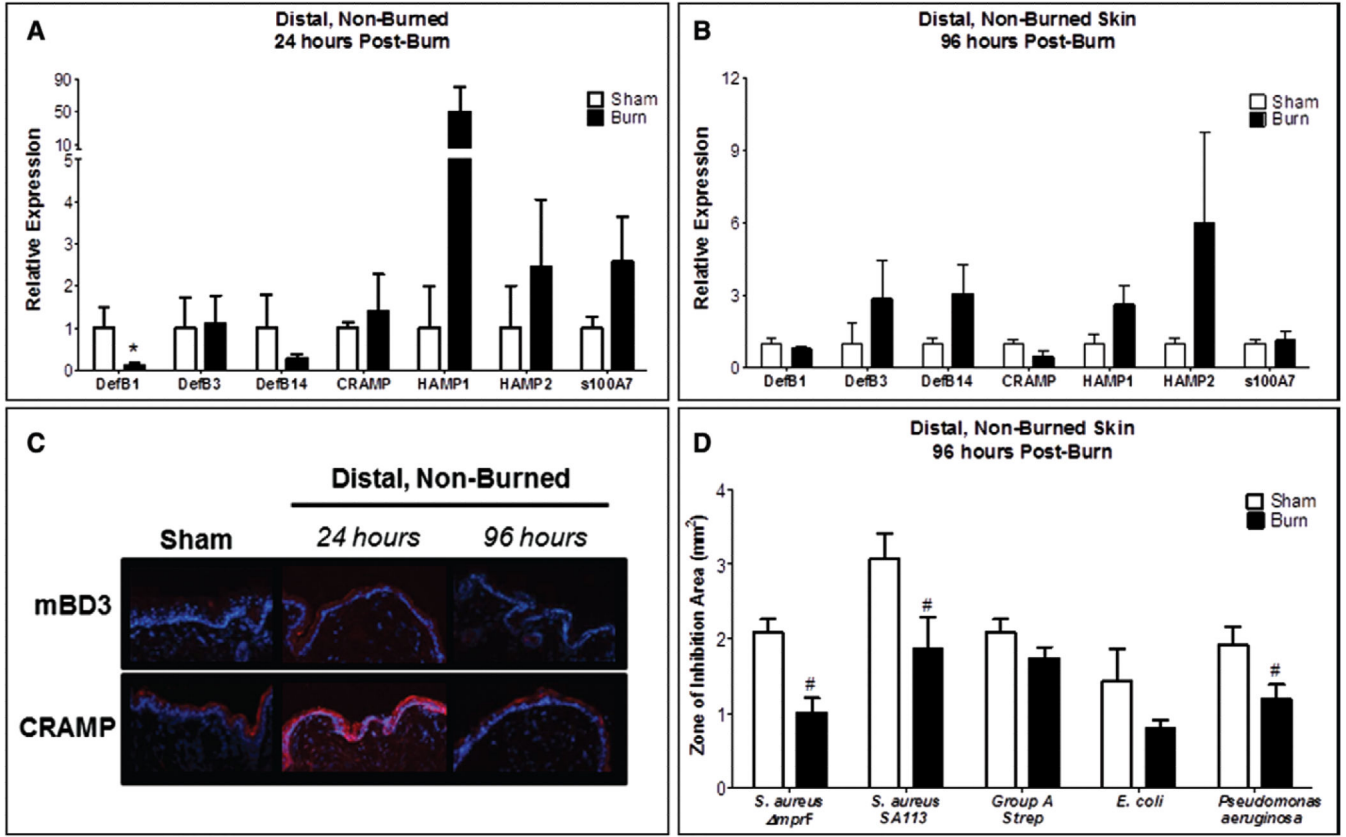


Figure 5. Local burn injury alters antimicrobial peptide production in distal unburned skin and reduces its capacity to restrict bacterial growth. Gene expression of *DefB1*, *DefB3*, *DefB14*, *Cramp*, *HAMP1*, *HAMP2*, and *s100A7* in distal skin at 24 hr (A) and 96 hr (B) postburn. $n = 3-8$ samples/group. Data analyzed by Mann-Whitney ($*p = 0.057$) and unpaired t test ($\#p < 0.05$). C, Distal skin was stained by immunohistofluorescence for mouse β -defensin 3 (mBD3) and cathelicidin-related antimicrobial peptide (CRAMP). $n = 3-4$ samples/group. D, Distal skin was harvested at 96 hr postburn and subjected to high-pressure liquid chromatography fractionation and radial diffusion assay. Bacterial growth inhibition was assessed for using ImageJ software. $n = 3-7$ samples/group. Data analyzed by unpaired t test ($\#p < 0.05$).

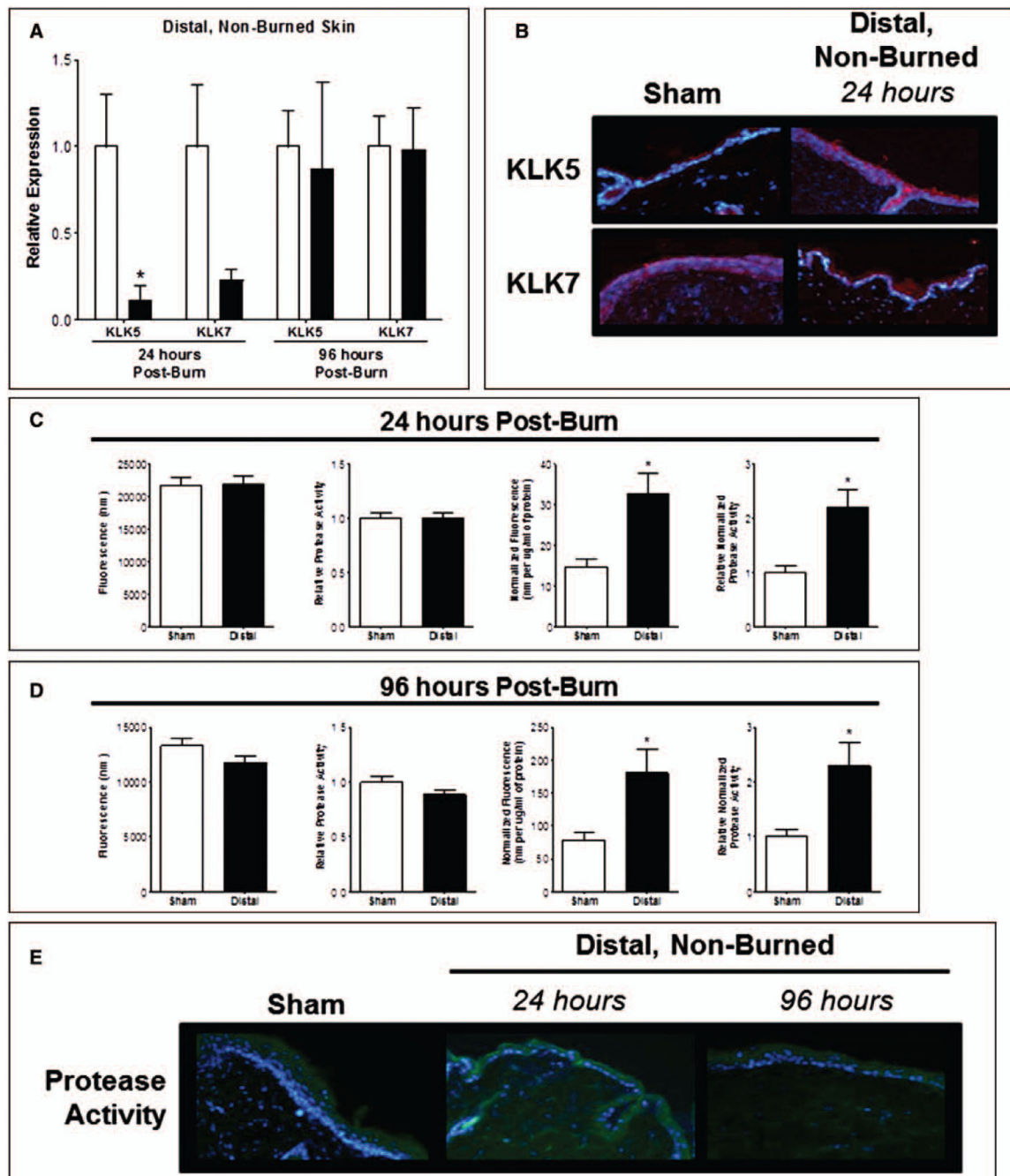


Figure 6. Protease activity is altered in distal, unburned skin after local burn injury. **A**, Gene expression of kallikrein (*KLK*) 5 and *KLK*7 in distal skin at 24 and 96 hr postburn. $n = 3-6$ samples/group. Data analyzed by unpaired t test ($*p < 0.05$). **B**, Distal skin was stained by immunohistofluorescence (IHF) for *KLK*5 and *KLK*7 at 24 hr postburn. $n = 3-4$ samples/group and performed in duplicate. Protease activity at 24 hr (**C**) and 96 hr (**D**) postburn using the EnzChek Protease Assay. Data expressed as raw fluorescence observed and normalized to protein concentration. $n = 6-7$ samples/group. Data analyzed by unpaired t

test ($*p < 0.05$). **E**, Protease activity in distal skin at 24 and 96 hr postburn by IHF at 20× magnification. $n = 3-4$ samples/group.